Pressure-induced spin reorientation and spin state transition in SrCoO_{3}

J.-Y. Yang, C. Terakura, M. Medarde, J. S. White, D. Sheptyakov, X.-Z. Yan, N.-N. Li, W.-G. Yang, H.-L. Xia, J.-H. Dai, Y.-Y. Yin, Y.-Y. Jiao, J.-G. Cheng, Y.-L. Bu, Q.-F. Zhang, X.-D. Li, C.-Q. Jin, Y. Taguchi, Y. Tokura, and Y.-W. Long

Phys. Rev. B **92**, 195147 — Published 24 November 2015

DOI: 10.1103/PhysRevB.92.195147

Pressure-induced spin reorientation and spin state transition in $SrCoO_3$

J.-Y. Yang,[1] C. Terakura,[2] M. Medarde,[3] J. S. White,[3] D. Sheptyakov,[3] X.-Z. Yan,[4] N.-N. Li,[4] W.-G. Yang,[4,5] H.-L. Xia,[1] J.-H. Dai,[1] Y.-Y. Yin,[1] Y.-Y. Jiao,[1] J.-G. Cheng,[1] Y.-L. Bu,[6] Q.-F. Zhang,[6,] X.-D. Li,[7] C.-Q. Jin,[1,8] Y. Taguchi,[2] Y. Tokura,[2,9] and Y.-W. Long[1,8,*]*

[1]Beijing National Laboratory for Condensed Matter Physics, Institute of Physics, Chinese Academy of Sciences, Beijing 100190, China

[2]RIKEN Center for Emergent Matter Science (CEMS), Wako 351-0198, Japan

[3]Laboratory for Neutron Scattering and Imaging, Paul Scherrer Institut, CH-5232 Villigen, Switzerland

[4]Center for High Pressure Science and Technology Advanced Research, 1690 Cailun Road, Shanghai 201203, P.R. China

[5]High Pressure Synergetic Consortium, Geophysical Laboratory, Carnegie Institution of Washington, 9700 S. Cass Ave, Argonne, IL 60439, USA

[6]Key Laboratory for Advanced Technology in Environmental Protection of Jiangsu Province, Yancheng Institute of Technology, Yancheng 224051, China

[7]Beijing Synchrotron Radiation Facility, Institute of High Energy Physics, Chinese Academy of Sciences, Beijing 100039, China

[8]Collaborative Innovation Center of Quantum Matter, Beijing 100190, China

[9]Department of Applied Physics, University of Tokyo, Tokyo 113-8656, Japan

PACS: 61.50.Ks, 71.15.Mb, 75.25.-j, 75.50.-y

*Corresponding Email: ywlong@iphy.ac.cn; qfangzhang@gmail.com

ABSTRACT

A series of high-pressure measurements including resistivity, ac/dc magnetic susceptibility, neutron powder diffraction and synchrotron x-ray diffraction were performed to investigate the crystal structure and electronic states of the itinerant ferromagnet $SrCoO_3$. Two pressure-induced phase transitions were observed at about 1.1 GPa and 45 GPa, corresponding to a spin reorientation and a spin state transition, respectively, while the cubic crystal structure was stable with pressure up to 60.0 GPa. The origins of these electronic state changes are discussed and rationalized in the light of first-principles calculations.

I. INTRODUCTION

Cobalt-based oxides continue to attract great attention due to their versatile charge, spin, and orbital degrees of freedom as well as the associated fascinating physical properties such as giant magnetoresistance,[1-3] high-performance thermoelectricity,[4] unconventional superconductivity [5] and large linear magnetoelectric effect.[6] As is well known, the spin states of Co ions are strongly dependent on the subtle balance between the crystal field energy and the Hund's rule exchange. As a consequence, various spin states are observed in cobalt oxides.[7-15] Since external stimuli can change significantly such an energy balance, Co ions in real materials can display a series of interesting transitions between different spin states under different temperature and pressure conditions. A well-known example is the low spin (LS) to high spin (HS) variation via a possible intermediate spin (IS) state that is observed in the rhombohedral perovskite $LaCoO_3$ with increasing temperature.[16-21] In addition, $Pr_{0.5}Ca_{0.5}CoO_3$ exhibits a pressure induced IS to LS transition, leading to a coherent change between a magnetic state with metallic conduction and paramagnetic insulating state.[22] Moreover, pressure-induced crystal structural and spin state phase transitions have also been found in other Co oxides such as $BiCoO_3$ and $SrRu_{0.5}Co_{0.5}O_3$, *etc*.[23,24]

In Co-based perovskite oxides, $SrCoO_3$ stands out due to its undistorted cubic perovskite structure with space group *Pm*-3*m* as well as the strong ferromagnetic (FM)

interaction with a high Curie temperature (T_C) above room temperature (~305 K measured for a single crystal in a field of 0.5 T).[12,13] Although the spin state of Co^{4+} in $SrCoO_3$ has been a subject of active debate, recent experimental studies on high-quality single crystals provide convincing evidence for the IS state,[12] in accordance with atomic multiplet theoretical calculations based on the Co-2*p* x-ray absorption spectrum.[25,26] Moreover, theoretical analysis has revealed that: 1) there exist strong *p*-*d* hybridizations and oxygen-hole effects due to the large negative charge-transfer energy between O-2*p* and Co-3*d* orbitals; 2) The electronic configuration of the Co^{4+} ion with IS state has a ground state consisting of 8% d^5, 67% $d^6\underline{L}$, and 25% $d^7\underline{L}^2$, where the $\underline{L}$ represents an oxygen hole; 3) The FM metallic state of $SrCoO_3$ mainly originates from the strong coupling between the itinerant oxygen holes and the high-spin Co-3d^6 ions (*i.e.* the dominant configuration $d^6\underline{L}$). The presence of the IS state in $SrCoO_3$ is thus indicative of the competing crystal field and Hund's-rule interactions, the relative strength of which can be tuned by external perturbations. It is therefore interesting to study pressure effects on the magnetism and spin state of $SrCoO_3$. In this paper, we performed a wide variety of high-pressure measurements such as ac/dc magnetic susceptibility, electric resistivity, neutron powder diffraction (NPD) and synchrotron x-ray diffraction (SXRD) as well as theoretical calculations to characterize the structure and electronic properties of $SrCoO_3$ under high pressure. Two pressure-induced magnetic transitions, namely, a spin reorientation and a spin-state transition were observed at different pressures.

II. EXPERIMENTAL AND CALCULATION DETAILS

High-quality $SrCoO_3$ was prepared by a two-step method as described in detail in Ref. 12. Oxygen content was found to be almost stoichiometric (2.95 ± 0.02) by a thermogravimetric analysis.[12] Pressure dependent resistivity (ρ) and ac magnetic susceptibility (χ_{ac}) were measured using a cubic-anvil-type high pressure apparatus at room temperature and under zero magnetic field. The temperature and field dependent dc magnetic susceptibility (χ_{dc}) measurements were carried out on a commercial superconducting quantum interference device magnetometer (Quantum Design) at

various pressures. The pressures were generated by a piston-cylinder high pressure system with glycerin as pressure transmitting medium. The pressure values were calibrated based on the superconducting transition temperature of metallic Pb.

The high pressure (P < 5.4 GPa) NPD measurements were carried out using a Paris-Edinburgh cell installed at the HRPT high-resolution diffractometer in the Swiss Spallation Neutron Source (SINQ), Paul Scherrer Institute.[27] The measurements were conducted at 200 K，a temperature at which the pressure can still be considered as hydrostatic, and using a neutron wavelength λ = 1.4931 Å. NaCl was mixed in with the powder sample and the observed pressure-dependence of its cubic lattice parameter was used to calibrate the applied sample pressure. A 4:1 mixture of deuterated methanol-ethanol was used as pressure transmitting medium. The NPD data was analyzed using the Rietveld package FULLPROF SUITE.[28] The primary room-temperature high pressure SXRD characterization was performed at the Beijing Synchrotron Radiation Facility, followed by detailed measurements under high pressure conducted at the beamline 16BM-D in the Advanced Photon Source, Argonne National Laboratory. The wavelength used for SXRD measurements was λ = 0.3099 Å. Pressure was generated by a diamond anvil cell with a pair of 300 μm culet anvils. Neon gas was used as pressure transmitting medium and the pressure values were calculated by the ruby fluorescence method. The SXRD data were analyzed using the Rietveld refinement program GSAS.[29]

First-principles calculations based on density functional theory (DFT) were performed for $SrCoO_3$. We used the generalized gradient approximation and the projected augmented wave method with a plane wave basis set as implemented in the Vienna ab initio Simulation Package.[30-32] A kinetic energy cut off was set to be 500 eV for the plane wave basis and the structural optimization was sampled with 16×16×16 Monkhorst-Pack k-point grid in combination with the tetrahedron method. All coordinates of atomic positions of $SrCoO_3$ were fully relaxed until the forces became small than 0.01 $eVÅ^{-1}$. The convergence of our calculations was checked carefully. The Wannier projection on DFT-calculated Co-*d* Bloch waves was performed with the VASP2WANNIER90 interface employing WANNIER90 for

constructing maximally localized Wannier orbitals. Through the Wannier projection, we obtained all hopping terms, crystal field energies and constructed a tight-binding Hamiltonian, which exactly reproduced the DFT-calculated Co-*d* bands. Magnetic anisotropy energies under pressures were calculated by non-collinear DFT, where spin-orbit coupling interactions were taken into account.

III. RESULTS AND DISCUSSION

Figure 1(a) shows the pressure dependence of the resistivity and the ac magnetic susceptibility of $SrCoO_3$ measured at zero field and room temperature. With increasing pressure, both the ρ and χ_{ac} exhibit an anomaly at a critical pressure (P_{C1}) about 1.1 GPa, indicating the occurrence of a pressure-induced variation in the magnetic and/or electronic properties (as shown later, the crystal structure remains unchanged). To further characterize this phase transition, dc magnetization was measured at different pressures. Based on the temperature dependent magnetization measured at 0.1 T shown in Fig. 1(b), we find that the FM Curie temperature almost linearly increases with pressure at a rate of ~13 K/GPa (see the inset), revealing that pressure enhances the FM double-exchange interaction occurring between Co-3d^6 electrons and oxygen holes. Note that the T_C value observed here at ambient pressure is slightly lower than that reported in Ref. 12. This is partly due to the difference in the magnetic field value (0.5T and 0.1T) used for the estimate of T_C. In addition, the temperature dependent magnetization exhibits different features below and above P_{C1}. When pressure is applied below P_{C1} (*e.g.* at 0.48 and 0.82 GPa), the magnetization shows a smooth temperature dependence below T_C. In sharp contrast, when the applied pressure is close to or larger than P_{C1} (*e.g.* at 1.04 and 1.28 GPa), the magnetization experiences a clear drop at a temperature T_{SR} (spin reorientation temperature) which increases with pressure. At the first glance, one may attribute this variation to a possible spin state transition as observed in many other cobalt oxides. However, if we check the field dependent magnetization, the saturated magnetic moments obtained both below and above P_{C1} are almost identical (see the inset of Fig. 1(c)), in contrast with the behavior expected for the occurrence of a spin-state

transition at this critical pressure. Furthermore, above P_{C1}, when the low-field magnetization is examined in detail, one can find an *S*-shaped metamagnetic behavior below T_{SR}, whereas canonical magnetization curve is observed above T_{SR}, as represented in Fig. 1(c). These observations could suggest that the easy magnetization axis of $SrCoO_3$ changes under high pressure, giving rise to a spin reorientation transition as will be demonstrated by our theoretical calculations.

In the case of a spin-state transition, changes in both, the Co-O interatomic distances and the value of Co magnetic moment are expected. Neutron powder diffraction is a desirable technique for this kind of investigation because it can obtain these parameters simultaneously. We therefore performed high-pressure NPD at 200 K ($< T_{SR}$) at pressures both below and above P_{C1} to get additional insight concerning the origin of the pressure-induced phase transition observed around 1.1 GPa. As shown in Fig. 1(b), the Co^{4+} moment is nearly saturated at 200 K and the saturation will most likely be maintained under the application of pressure taking into account the linear increase of Curie temperature T_C with P. Since the intensity of magnetic reflections is proportional to the square of the ordered Co^{4+} magnetic moment, any change in moment will be easier to detect at 200 K than at room temperature, where the ordered magnetic moment is about 1/3 of the saturation value. Figures 2(a) and 2(b) show the Rietveld refinements of the NPD patterns obtained at ambient pressure ($< P_{C1}$) and 5.4 GPa ($> P_{C1}$), respectively. The pressure dependence of unit cell volume obtained from such refinements is shown in Fig. 2(c). In other cobalt oxides such as $BiCoO_3$[23] or $GdBaCo_2O_{5.5}$[33], a spin-state transition from a higher to a lower spin state has been shown to lead to a discontinuous shrinking in unit cell volume. In the present case, however, the unit cell volume smoothly decreases with increasing pressure, and no obvious anomaly is observed up to the highest pressure value 5.4 GPa used in this experiment. The volume−pressure relationship can be well fitted based on the Birch-Murnaghan equation of state with $P = 1.5\times B_0\times(x^{-7/3}-x^{-5/3})\times[1+0.75(B'-4)\times(x^{-2/3}-1)]$ (see Fig. 2(c)). Here $x = V/V_0$ is the normalized volume, V_0 is the unit cell volume at pressure $P = 0$ GPa, and B_0, B' the bulk modulus and its derivative with respect to the pressure. The fitted value of B_0 is 144 ± 2 GPa with

fixed $B' = 4$. A further argument supporting the absence of spin-state transition at 1.1 GPa is that the magnetic contribution to the Bragg reflections is found to be nearly unchanged with pressure up to 5.4 GPa. As a consequence, the refined value of the Co^{4+} magnetic moment shown in Fig. 2(c), takes a nearly constant value very close to ~ 1.7 μ_B, compatible with both a highly-hybridized IS spin state and the results of the magnetization measurements (see Fig. 1(b)).[12] Our high pressure NPD results thus solidly confirm both the stability of the crystal structure and the spin state of $SrCoO_3$ below 5.4 GPa.

In order to explore the possible spin state transition at much higher pressure, SXRD was carried out at room temperature for sample pressures up to 60.0 GPa. Figure 3(a) shows some typical SXRD patterns collected at selected pressures. As the pressure increases, the peak positions systematically shift to higher diffraction angles due to the volume compression, and no structural phase transformation is observed even when the pressure is increased to 60.0 GPa. Figure 3(b) shows the Rietveld structure refinement at a representative pressure 46.0 GPa, at which the SXRD pattern can still be well fitted on the basis of a simple cubic perovskite structure with space group *Pm*-3*m*. However, when the pressure dependence of the unit cell volume is examined as shown in Fig. 3(c), a clear anomaly is observed at another critical pressure P_{C2} around 45 GPa. The change of spin state in other cobalt perovskite oxides is accompanied by an anomaly in unit cell volume and/or Co-O interatomic distances due to the different ionic radii at different spin states even in the case of no change of crystal symmetry.[21,24,34] Thus, the anomaly at P_{C2} suggests the occurrence of a spin state variation from IS to LS in $SrCoO_3$. According to the Birch-Murnaghan equation of state mentioned above, the room-temperature bulk modulus below P_{C2} is fitted to be 164 ± 4 GPa, which is comparable to those observed in most perovskite oxides.[35-37] Above P_{C2}, however, the bulk modulus B_0 considerably increases to 229 ± 19 GPa. In other cobalt perovskite oxides, the pressure-induced spin state transition also gives rise to a sharp increase in B_0.[36] In comparison, the anomaly in unit cell volume and the significant increase of B_0 in the present $SrCoO_3$ sample may suggest the occurrence of a pressure-induced spin state transition from IS to LS. Note that since the unit cell

volume of $SrCoO_3$ does not show a first-order-like drop with pressure across P_{C2}, the associated IS-LS transition is more likely continuous over a wider pressure region (36.8-46.0 GPa) as shown in Fig. 3(c).

To get deeper insight on the pressure effects on the magnetic state in the present cubic perovskite $SrCoO_3$, first-principles calculations based on density functional theory were performed. Figure 4(a) shows the pressure-dependent crystal field energy (10 Dq) and p-d transfer interaction ($|t|$) between Co-3d and O-2p orbitals. Obviously, both of them increase with increasing pressure. As mentioned above, the FM interaction of $SrCoO_3$ mainly originates from the double exchange between the Co-3d^6 electrons and oxygen holes in the dominant $d^6\underline{L}$ configuration. Clearly, the pressure can enhance the p-d transfer interaction significantly (Fig. 4(a)). As a result, the FM Curie temperature of $SrCoO_3$ increases with increasing pressure consistent with experimental observation (Fig. 1(b)). On the other hand, the crystal field energy also increases with elevating pressure which can result in a spin state transition if the pressure is high enough. Actually, when we check the total system energy as a function of pressure for the IS and LS states, respectively, we can find a crossover around 50 GPa where IS and LS states are strongly mixed and the transition of spin state from IS to LS is completely achieved by using higher pressure as shown in Fig. 4(b). This supports the pressure-induced and continuous-like spin-state transformation as suggested by the SXRD experiments (Fig. 3(c)). Also we calculated the pressure dependence of unit cell volume, and found that the bulk modulus significantly increases from $B_0 = 166 \pm 2$ GPa to $B_0 = 194 \pm 2$ GPa across $P = P_{C2}$. This result is qualitatively in accordance with the experimental result (Fig. 3(c)).

Furthermore, we calculated the energy difference with easy magnetization axis along [110] and [111] directions relative to the [100] direction under high pressure. As shown in Fig. 4(c), the [111] direction is favorable in energy at lower pressures. However, when pressure increases to about 3.7 GPa, the [100] direction becomes more stable in energy. Therefore, the anomalous variations observed in resistivity, ac and dc magnetic susceptibility curves near P_{C1} (see Fig. 1) may be attributed to a pressure induced spin-reorientation transition.

IV. CONCLUSIONS

In summary, pressure effects on the crystal structure and the Co^{4+} spin state were studied in detail for $SrCoO_3$ single crystals using different experimental techniques and first-principles calculations. The FM Curie temperature of $SrCoO_3$ increases with pressure due to an enhancement of the FM double-exchange interaction between Co-3d^6 electrons and oxygen holes. Although the cubic perovskite structure of $SrCoO_3$ is stable with pressure up to 60.0 GPa, two pressure-induced changes in the electronic system are observed at 1.1 GPa and 45 GPa. The first of them is attributed to a spin reorientation due to a pressure-driven change of the easy magnetization axis, whereas the second one is most likely a pressure-induced spin state transition. In contrast with the first-order spin-state transitions observed in most cobalt oxides, the present one appears to be continuous, and to occur over a wide pressure region.

ACKNOWLEDGMENTS

This work was supported by 973 Project of the Ministry of Science and Technology of China (Grants No. 2014CB921500, 2015CB921303), and the Strategic Priority Research Program of the Chinese Academy of Sciences (Grants No. XDB07030300, XDB07020200). Q. Zhang thanks the support by the NSFC (11474246, 11204265), Foundation of the Jiangsu Higher Education Institutions of China (13KJ430007) and the Qing Lan Project. HPCAT operations were supported by DOE-NNSA under Award No. DE-NA0001974 and DOE-BES under Award No. DE-FG02-99ER45775, with partial instrumentation funding by NSF. The gas loading was performed at GeoSoilEnviroCARS, APS, ANL, supported by EAR-1128799 and DE-FG02-94ER14466. APS was supported by DOE-BES, under Contract No. DE-AC02-06CH11357. The neutron experiments were performed at the Swiss spallation neutron source SINQ, Paul Scherrer Institute, Villigen, Switzerland.

REFERENCES

[1]G. Briceno, H. Chang, X. D. Sun, P. G. Schultz, X. D. Xiang, Science **270**, 273 (1995).

[2]C. Martin, A. Maignan, D. Pelloquin, N. Nguyen, and B. Raveau , Appl. Phys. Lett. **71**, 1427 (1997).

[3]A. Maignan, C. Martin, D. Pelloquin, N. Nguyen, and B. Raveau, J. Solid State Chem. **142**, 247 (1999).

[4]K. Fujita, T. Mochid, K. Nakamura, Jpn. J. Appl. Phys. **40**, 4644 (2001).

[5]K. Takada, H. Sakurai, E. Takayama-Muromachi, F. Izumi, R. A. Dilanian, T. Sasaki , Nature **422**, 53 (2003).

[6]V. Caignaert, A. Maignan, K. Singh, C. Simon, V. Pralong, B. Raveau, J. F. Mitchel, H. Zheng, A. Huq, and L. C. Chapon, Phys. Rev. B **88**, 174403 (2013).

[7]M. Oku, J. Solid State Chem. **23**, 177 (1978).

[8]Z. Hu, C. Mazumdar, G. Kaindl, F. M. F. de. Groot, S. A. Warda, D. Reinen, Chem. Phys. Lett. **297**, 321 (1998).

[9]Z. Hu, H. Wu, M. W. Haverkort, H. H. Hsieh, H. J. Lin, T. Lorenz, J. Baier, A. Reichl, I. Bonn, C. Felser, A. Tanaka, C. T. Chen, L. H. Tjeng, Phys. Rev. Lett. **92**, 207402 (2004).

[10]A. A. Belik, S. Iikubo, K. Kodama, N. Igawa, S. Shamoto, S. Niitaka, M. Azuma, Y. Shimakawa, M. Takano, F. Izumi, E. Takayama-Muromachi, Chem. Mater. **18**, 798 (2006).

[11]K. Yamaura, H. W. Zandbergen, K. Abe, R. J. Cava, J. Solid State Chem. **146**, 96 (1999).

[12]Y. W. Long, Y. Kaneko. S. Ishiwata, Y. Taguchi, Y. Tokura, J. Phys.: Condens. Matter **23**, 245601 (2011).

[13]Y. W. Long, Y. Kaneko, S. Ishiwata, Y. Tokunaga, T. Matsuda, H. Wadati, Y. Tanaka, S. Shin, Y. Tokura, and Y. Taguchi, Phys. Rev. B **86**, 064436 (2012).

[14]J. Matsuno, Y. Okimoto, Z. Fang, X. Z. Yu, Y. Matsui, N. Nagaosa, M. Kawasaki, Y. Tokura, Phys. Rev. Lett. **93**, 167202 (2004).

[15]R. Jin, H. Sha, P. G. Khalifah, R. E. Sykora, B. C. Sales, D. Mandrus, J. Zhang,

Phys. Rev. B **73**, 174404 (2006).

[16]M. A. Korotin, S. Yu. Ezhov, I. V. Solovyev, and V. I. Anisimov, Phys. Rev. B **54**, 5309 (1996).

[17]T. Saitoh, T. Mizokawa, A. Fujimori, M. Abbate, Y. Takeda, M. Takano, Phys. Rev. B **55**, 4257 (1997).

[18]K. Asai, A. Yoneda, O. Yokokura, and K. Kohn, J. Phys. Soc. Jpn. **67**, 290 (1998).

[19]S. Yamaguchi, Y. Okimoto, and Y. Tokura, Phys. Rev. B **55**, 8666(R) (1997).

[20]C. Zobel, M. Kriener, D. Bruns, J. Baier, M. Gruninger, and T. Lorenz, Phys. Rev. B **66**, 020402 (2002).

[21]P. G. Radaelli and S. W. Cheong, Phys. Rev. B **66**, 094408 (2002).

[22]P. Tong, Y. S. Wu, B. Kim, D. Kwon, J. M. Sungil Parak, and B. G. Kim, J. Phys. Soc. Jpn. **78**, 3 (2009).

[23]K. Oka, M. Azuma, W. Chen, H. Yusa, A. A. Belik, E. Takayama-Muromachi, M. Mizumaki, N. Ishimatsu, N. Hiraoka, M. Tsujimoto, M. G. Tucker, J. P. Attfield, Y. Shimakawa, J. Am. Chem. Soc. **132**, 9438 (2010).

[24]J. M. Chen, Y. Y. Chin, M. Valldor, Z. W. Hu, J. M. Lee, S. C. Haw, N. Hiraoka, H. Ishii, C. W. Pao, K. D. Tsuei, J. F. Lee, H. J. Lin, L. Y. Jang, A. Tanaka, C. T. Chen, and L. H. Tjeng, J. Am. Chem. Soc. **136**, 1514 (2014).

[25]R. H. Potze, G. A. Sawatzky, M. Abbate, Phys. Rev. B **51**, 11501 (1995).

[26]M. Zhuang, W. Y. Zhang, A. Hu, and N. B. Ming, Phys. Rev. B **57**, 13655 (1998).

[27]P. Fischer, G. Frey, M. Koch, M. Könnecke, V. Pomjakushin, J. Schefer, R. Thut, N. Schlumpf, R. Bürge, U. Greuter, S. Bondt, E. Berruyer, Physica B **146**, 276 (2000).

[28]J. Rodríguez-Carvajal, Physica B **192**, 55 (1993).

[29]A. C. Larson and R. B. Von Dreele, Los Alamos National Laboratory Report No. LAUR 86, 748, 1986 (unpublished).

[30]G. Kresse, J. Hafner, Phys. Rev. B **47**, 558 (1993).

[31]G. Kresse, J. Furthmüller, Phys. Rev. B **54**, 11169 (1996).

[32]P. E. Blöchl, Phys. Rev. B **50**, 17953 (1994).

[33]C. Frontera, J. L. García-Muñoz, A. Llobet, and M. A. G. Aranda, Phys. Rev. B **65**, 180405 (2002).

[34]Y. Ren, J. Q. Yan, J. S. Zhou, J. B. Goodenough, J. D. Jorgensen, S. Short, H. Kim, Th. Proffen, S. Chang, and R. J. McQueeney, Phys. Rev. B **84**, 214409 (2011).

[35]J. S. Zhou, C. Q. Jin, Y. W. Long, L.X. Yang，and J. B. Goodenough, Phys. Rev. Lett. **96**, 046408 (2006).

[36]J. S. Zhou, J. Q. Yan, and J. B. Goodenough, Phys. Rev. B **71**, 220103(R) (2005).

[37]M. Amboage, M. Hanfland, J. A. Alonso, and M. J. Martınez-Lope, J. Phys.: Condens. Matter **17**, 783 (2005).

Figures and figure captions:

FIG. 1. (a) Pressure dependence of resistivity and ac magnetic susceptibility measured at room temperature. (b) Temperature dependent dc magnetization measured at selected pressures. The inset shows pressure dependence of T_C. (c) Low-field isothermal magnetization measured at 1.28 GPa and different temperatures. The inset shows the magnetization measured at 2 K with field up to 7 T at various pressures.

FIG. 2. NPD patterns and Rietveld refinement results at (a) ambient pressure (AP) and (b) 5.4 GPa. Observed (red circle), calculated (black line) and difference (blue line) profiles are shown together with the allowed Bragg reflections of nuclear (top ticks), NaCl (middle ticks), and magnetic (bottom ticks) diffractions. (c) Unit cell volume and magnetic moment of Co^{4+} as a function of pressure. The red solid line is a fit to the volume data based on the Birch-Murnaghan equation of state.

FIG. 3. (a) Representative SXRD patterns collected at various pressures and room temperature. The asterisks stand for the diffraction peak originating from the pressure transmission medium Neon. (b) SXRD pattern and Rietveld refinement result at a typical pressure 46.0 GPa. Observed (black cross), calculated (red line) and difference (blue line) profiles are shown together with the allowed Bragg reflections (ticks). (c) Pressure dependence of unit cell volume. The red and blue solid lines are the fitting results to the volume data based on the Birch-Murnaghan equation of state below 36.8 GPa and above 46.0 GPa, respectively.

FIG. 4. (a) Pressure dependent crystal field splitting energy (10 Dq) and p-d transfer interaction ($|t|$). (b) Pressure dependence of total system energy for IS and LS states. (c) Relative energy for different spin orientations with respect to the energy for [100] orientation at different pressures.

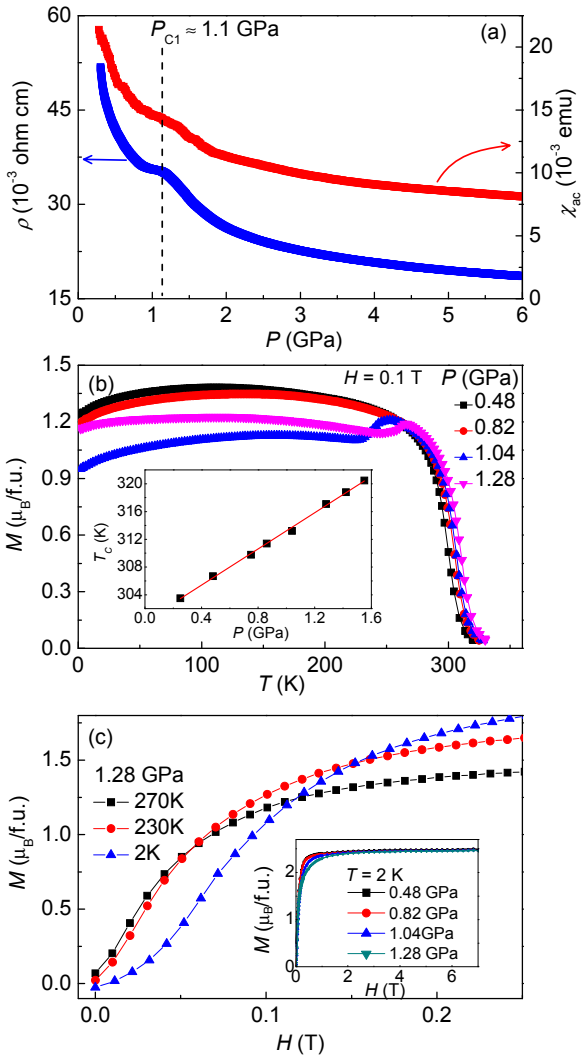

Figure 1

Yang *et al*

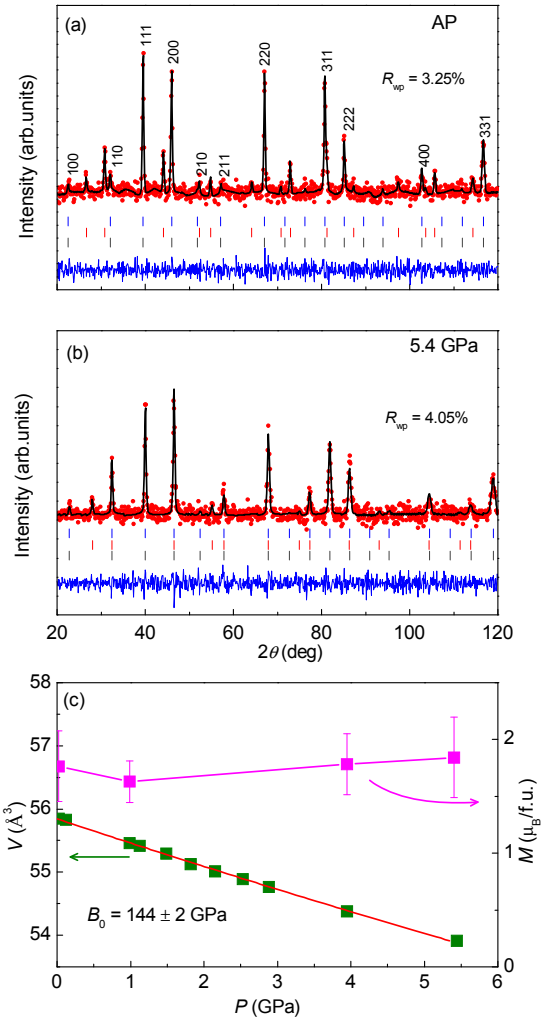

Figure 2

Yang *et al*

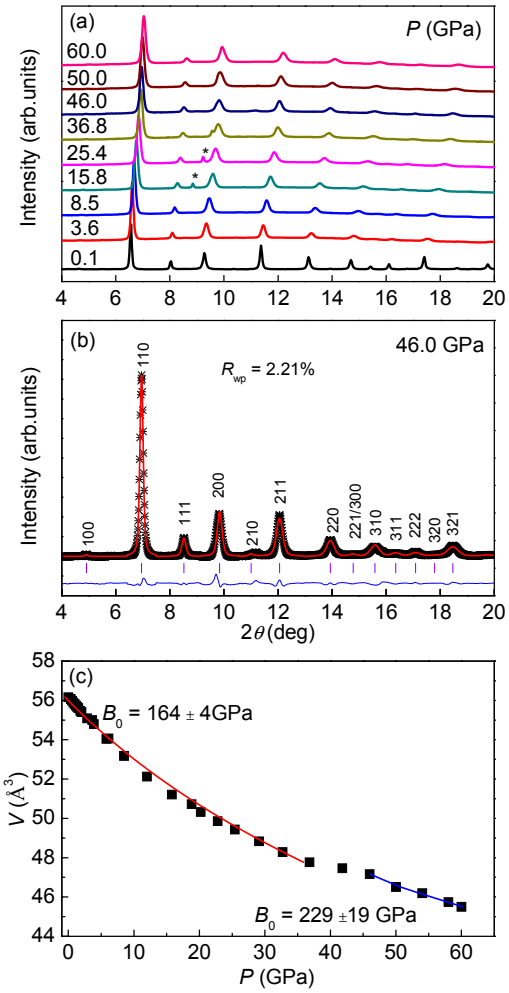

Figure 3

Yang *et al*

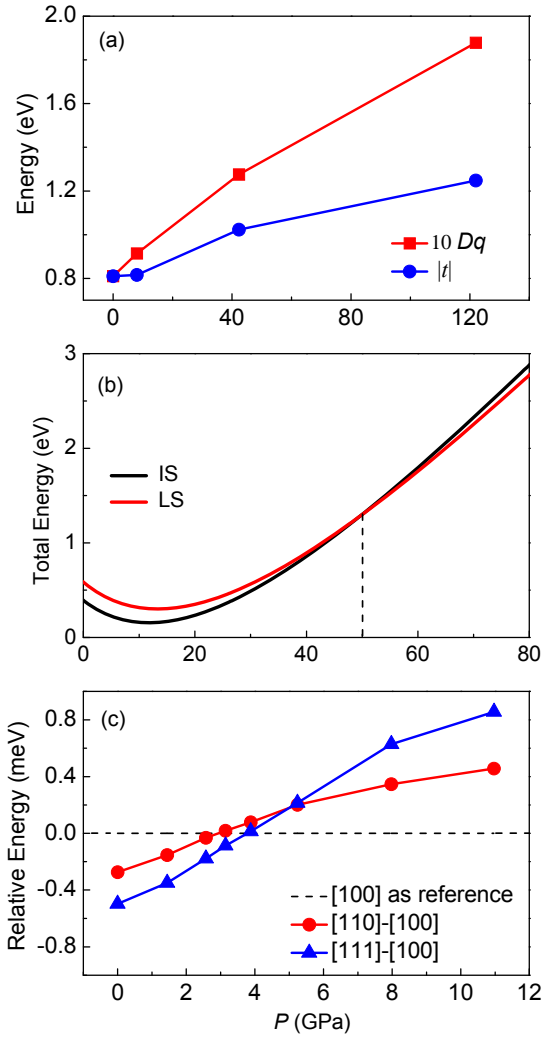

Figure 4

Yang *et al*